25th ABCM International Congress of Mechanical Engineering
October 20-25, 2019, Uberlândia, MG, Brazil

COBEM2019-0505
NUMERICAL AND EXPERIMENTAL STUDY OF A FLOW AROUND TWO CIRCULAR CYLINDERS IN A WIND TUNNEL

Jésus Fernandes Júnior
Weslley Albiani Alves
Vitor Lomeu Cerqueira
Cristiana Brasil Maia
Pontifícia Universidade Católica de Minas Gerais
Av. Dom José Gaspar, 500, Coração Eucarístico, Belo Horizonte – MG, Brasil. CEP 30535-610.
jesferjun@gmail.com
weslley.albiani@gmail.com
lomeuvitor@gmail.com
cristiana@pucminas.br

Abstract. *Great advances have been achieved over time, among them, the wind tunnel - an important tool for aerodynamic research - and Computational Fluid Dynamics techniques – where natural phenomena related to fluids can be modeled and dealt with through numerical methods. The flow around cylinders can be used to model a large variety of cases of flows. They occur in several studies involving numerical and experimental engineering due to their great occurrence in nature and technological applications. Flows around bridges, boats, buildings, trees, islands, aerodynamic geometries and heat exchangers are just a few examples of studies in the area. The objective of this work is the numerical and experimental analysis of the flow around two cylindrical bodies submerged in a stream of air in a wind tunnel. It was used the low speed wind tunnel of the Pontifical Catholic University of Minas Gerais. Numerical analyzes were performed using the Ansys - CFX ® 18.2 commercial program, with the κ - ω SST turbulence model, simulating the positions of the two cylinders in transient regimes. The experimental pressure was measurements at the wind tunnel outlet test section, using a static Pitot tube and two circular aluminum cylinders, diameter of 29.7 mm. The interference caused by the insertion of a second cylinder downstream of the first was analyzed. The pressure and velocity fields obtained indicate the stagnation and separation points in the cylinders. The pressure coefficients and shear stresses showed the detachment angles around 87° and 113° for first and second cylinders, respectively. Drag force of 0.196 N were found throughout the test section Numerical results were compared to experimental data and the model was considered validated.*

Keywords: *Wind tunnel, Turbulence, Cylinders, CFD, Flow around two circular cylinders*

1. INTRODUCTION

Wind tunnel is a fundamental instrument for aerodynamic designs and research that aims to simulate conditions of a flow not bounded by solid boundaries, although limitations on size of equipment make it unachievable in practice (FOX et al., 2010). On the other hand, we have a second approach: the resolution of differential or integral equations analytically or numerically. The basic equations of fluid motion are very difficult to allow the analyst to study arbitrary geometric configurations. It is possible to apply computational numerical techniques to complex geometries, this method knows as Computational Fluid Dynamics (CFD).

Vasconcellos (2015) performed a numerical and experimental study of the flow around a circular cylinder in the low speed wind tunnel Pontifical Catholic University of Minas Gerais - Puc Minas -, for a rotation of the blower of 2500 rpm. Using 36 measuring points and a hot wire anemometer, the velocity at the entrance and the outlet of the test section was measured through a Pitot tube. Experimental tests were made for the wind tunnel without a cylinder. With a cylinder and with a Helmholtz resonator. Turbulence models were evaluated three models of turbulence: standard k-ε, k-ω SST, and EARSM BSL (Algebraic Reynolds Number Algebraic Reynolds Number model). A volumetric flow 0.294 m³/s was found. Experimental results showed that the flow undergoes few changes upstream of the blunt body. The κ-ω turbulence models SST and BSL EARSM stood out in relation to the κ-ε turbulence model, presenting closer results. The thickness of the boundary layer found at the entrance was slightly greater than 5 mm and slightly larger than 19 mm at the exit. The k-ω SST model accounted for a thickness of 20.60 mm and the EARSM BSL, 20.10 mm. The standard k-ε model showed 6.75 mm at the entrance and 22.61 mm at the exit, observing that the flow was not completely developing inside the

tunnel. The author found volumetric flow 0.239 m³/s at the entrance and 0.244 m³/s at the output (one cylinder inside the test section). That difference is there attributed to the difficulties of correctly positioning the Pitot static probe.

Lana (2017) numerically studied the flow behavior around a cylinder at different fluid velocities. For the simulations tests, the commercial program Ansys CFX® 17.0 used, with rotations of 1800 rpm, 2300 rpm, 2700 rpm and 3200 rpm. The author observed that the coefficient of friction is zero around 80°. The values obtained for the thicknesses of the boundary layers: $\delta = 0.0062$m, for 1800 rpm; $\delta = 0.0055$m, at 2300 rpm; $\delta = 0.0051$m, at 2700 rpm; $\delta = 0.0047$m, at 3200 rpm. Since the test section of the wind tunnel has equal edges of 0.20m, it can be state that the flow is completely developed. Was found the maximum velocity around the cylinder in the separation region.

Xiang et al. (2017) studied in a wind tunnel moving vehicles under side winds through a new approach, where a device adjusts wind directions and their angles of attack. The coefficients of five components of the vehicle model movement tested with the force balance equipment. The results showed that the vehicle in motion and the proposed device could provide a soft wake at its point of stagnation. Aerodynamic strength and momentum are stable after filtration, with aerodynamic characteristics identified for different wind speeds.

Teo et al. (2018) studied additional wind tunnel components in a wind tunnel to analyze the physical distortions associated with these components, as well as the procedures adopted to correct them. The wing deflections observed during the test were quantified by image process and incorporated into numerical simulations. These results agreed with the wind tunnel measurement results. The authors concluded that these wing components tested are more economical and have fast turnaround time.

Hill et al. (2018) examined potential reductions in wind tunnel testing requirements. The authors cite that for tests in wind tunnels a large number of experimental data is necessary, which can consume time and resources. They proposed an improvement in the efficiency of wind tunnel testing through experimental design, which compares data resulting from a survey of wind tunnel tests and data generated by this experimental design, as it called.

The interference caused by the presence of more than one body in the flow domain is responsible for changes both in the characteristics of the forces imposed on the bodies by the fluid and in the resulting velocity field. Investigations around cylinders can provide a better understanding of vortex dynamics, pressure distribution, and fluid forces in more complex cases. The present article aims to evaluate the flow around two circular cylinders placed in the section of tests of a wind tunnel, for a blower rotation of 2500 rpm. A comparison between experimental and numerical methods is presenting, as well as results for velocity and pressure, pressure coefficient, shear stress and displacement of the boundary layer of both cylinders.

2. METHODOLOGY

For both tests, experimental and numerical, two cylinders made of aluminum with 29.7 mm of diameter and 200 mm of length were used. Cylinder 1 was positioned in the middle of the test section, 470 mm from its entrance; cylinder 2 was positioned at 77.22 mm from the first, in a zone of proximity and wake interference, Fig. 1, according to Zdravkovich's study (1984 and 1988).

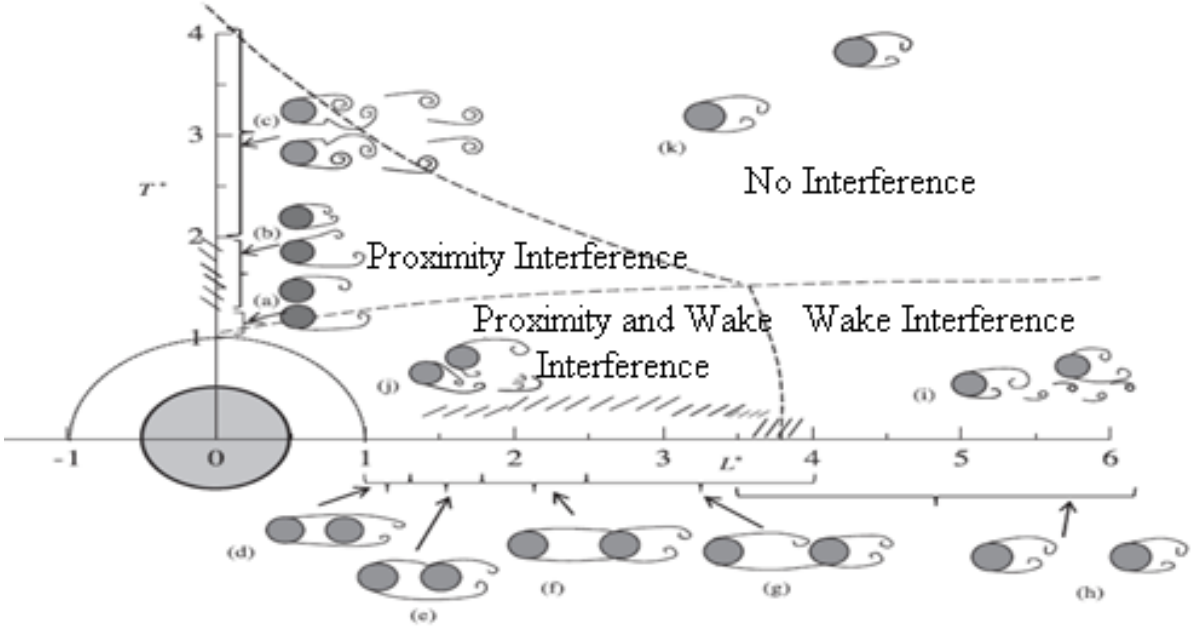

Figure 1. Interference-based flow classification.
Adapted from Zdravkovich, 1984.

In the experimental test, a low-velocity wind tunnel was used, as shown in Fig. 2. Pressure data was determined through a Prandtl type pitot tube and a liquid column differential manometer. Subsequently, pressure was used to determinate the velocity.

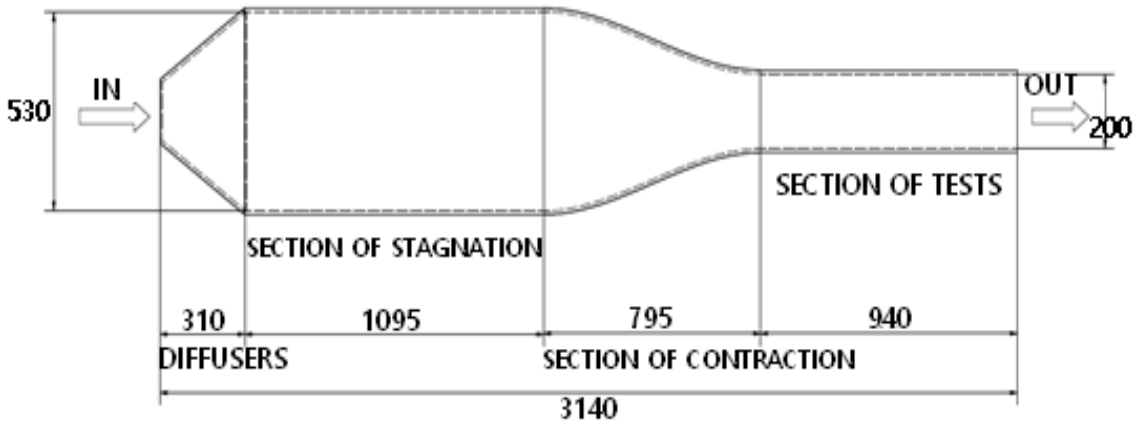

Figure 2. Schematic drawing of the studied wind tunnel [mm].

The physical dimensions and boudary conditions were obtained from experimental data for a low speed wind tunnel at the Pontifical Catholic University of Minas Gerais, Belo Horizonte. The section of tests of the wind tunnel in question is square, with 200 mm of edge and 940 mm of length and the solution domain is presenting in Fig. 3.

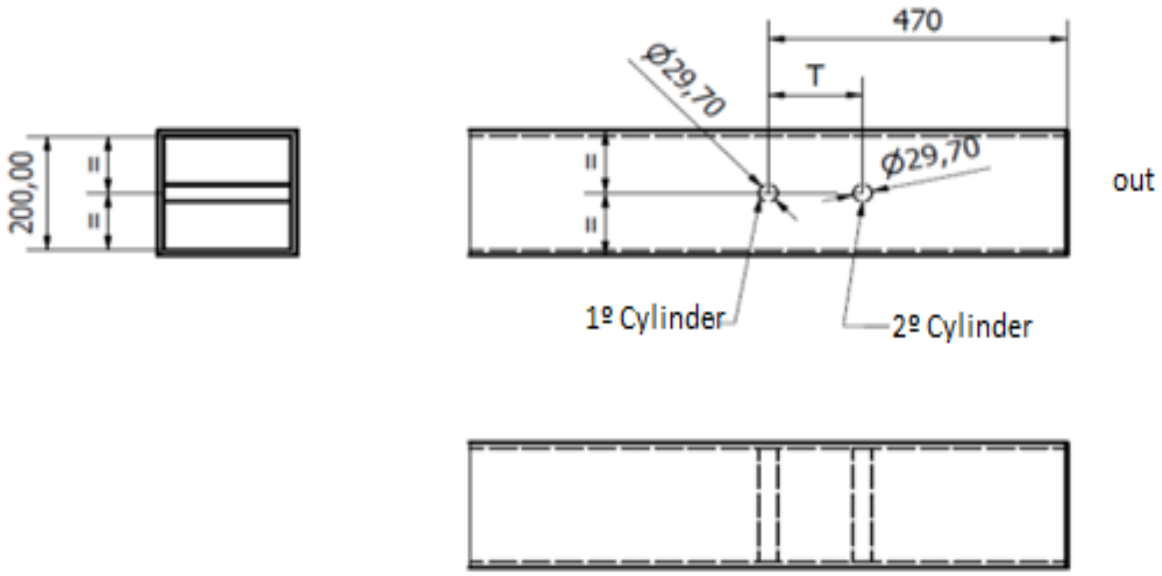

Figure 3. Positioning the cylinders in the test section

The blower has been adjusting to a rotation of 2500 rpm. The first measurement was performed after five minutes of operation of the blower. Two other measurement were performed in an interval of three minutes. At each reading, data of dynamic pressure, barometric pressure and ambient temperature has collected.

Following study of Soares (2008), the section of tests was mapped, having as reference the standard ISO 3966: 2008 (identical to ISO 3966: 2013), which defines the points as a function of the dimension of the lateral edge for a rectangular duct by the log-Chebyshev method. Figure 4 shows the 36 measurement points.

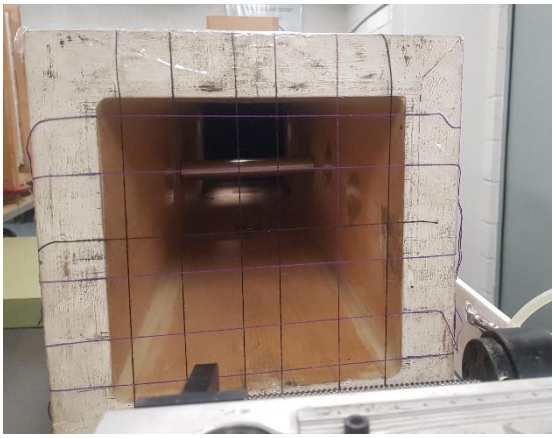

Figure 4. Wind tunnel with mapped test section output.

For simulations of this work, a computer with Windows® 10 64-bit operating system, Intel® Core i7 7700HQ processor with 2.8 GHz of base clock, 3.8 GHz of maximum clock frequency, 16 GB RAM and a Nvidia® GEFORCE® GTX 1050ti graphics card was used. The numerical analysis was performed using the commercial software Ansys CFX® 18.2.

The fundamental hypotheses and boundary conditions adopted are air as ideal gas, flow in unsteady state, isothermal flow at 20º C, output with relative static pressure of 0 Pa, waterproof walls, non-slip condition for wind tunnel walls and cylinder walls, mass flow rate of 0.294 kg/s at input - based on experimental results, turbulent intensity of 5, turbulence model κ-ω SST (Shear Stress Transport) and timestep based on Strouhal number equal to 0.002.

2.1 Mathematical models

According to Gusberti et al. (2004), the κ-ω SST (Shear Stress Transport) model devised to provide highly accurate predictions of onset and amount of runoff separation under adverse pressure gradients through the inclusion of transport effects in the formulation of turbulent viscosity.

Wilcox (2000) proposed κ-ω model of Wilcox, which is suitable for external flows and general purposes in CFD. According to Versteeg and Malalasekera (2007), it is a model that predicts with great virtue what happens in the regions near the walls. On the other hand, it is inappropriate to use in free flowing.

Eq. (1), mass conservation equation, establishes that the time variation of mass per unit volume, (kg/s.m3), within the infinitezimal control volume is equal to the spatial variation of mass flow per unit of time, (kg/s.m3), which crosses the control surface (White, 2011).

$$\frac{\partial}{\partial t}\rho + \nabla.\vec{V} = 0 \tag{1}$$

The most general form of the Navier-Stokes equation is presented at Eq. (2).

$$\frac{\partial}{\partial t}\left(\rho\vec{V}\right) + \nabla.\left(\rho\vec{V}\vec{V}\right) = -\nabla p - \frac{2}{3}\nabla\left(\mu\nabla\vec{V}\right) + \nabla.(2\mu S) + \rho\vec{g} \tag{2}$$

Menter (1992) proposed the κ-ω SST model, which is also a model of two transport equations. It is a review of the κ-ε and κ-ω models. The results of the κ-ε model did not vary so much for values assumed in the free flow; however, in regions close to the walls, this model was unsatisfactory for boundary layers subjected to pressure gradients.

Versteeg and Malalasekera (2007) also showed that for the turbulence model k-ω SST the calculation of the Reynolds and the turbulent kinetic energy of the system is the same as that used for the standard κ-ε model, but the dissipation rate of the kinetic energy were transformed into the dissipation frequency, which can be seen in Eq. (3).

$$\epsilon = \kappa.\omega \tag{3}$$

$$\frac{\partial(\rho k)}{\partial t} + \frac{\partial(\rho k u)}{\partial x} + \frac{\partial(\rho k v)}{\partial y} + \frac{\partial(\rho k w)}{\partial z} = \left(\mu + \frac{\mu_t}{\sigma_{k,1}}\right)\left(\frac{\partial^2 k}{\partial x^2} + \frac{\partial^2 k}{\partial y^2} + \frac{\partial^2 k}{\partial z^2}\right) + 2\mu_t S_{ij}.S_{ij} - \rho\omega \tag{4}$$

$$\frac{\partial(\rho\omega)}{\partial t}+\frac{\partial(\rho\omega u)}{\partial x}+\frac{\partial(\rho\omega v)}{\partial y}+\frac{\partial(\rho\omega w)}{\partial z}=\left(\mu+\frac{\mu_t}{\sigma_{\mu,1}}\right)\left(\frac{\partial^2\omega}{\partial x^2}+\frac{\partial^2\omega}{\partial y^2}+\frac{\partial^2\omega}{\partial z^2}\right)+\gamma_2\left(2\rho S_{ij}.S_{ij}--\frac{2}{3}\rho\varpi\frac{\partial U_i}{\partial x_j}S_{ij}\right)-\beta_2\rho\varpi+2\frac{\rho}{\sigma_{\varpi,2}\omega}\frac{\partial k}{\partial x_k}\frac{\partial\omega}{\partial x_k} \quad (5)$$

A cylinder immersed in a stream of fluid experiences a drag force given by Eq. (6) (Fox, Pritchard and McDonald, 2010):

$$F_a = C_A.\frac{\rho V_\infty^2}{2}.A \quad (6)$$

In the Eq. (6), A represents the front area of the cylinder, C_A the drag coefficient and V_∞ represents the free flow velocity.

To predict the point of separation of the flow around a circular cylinder by calculating the pressure coefficient, given by Eq. (7) (White, 2011):

$$C_P = \frac{P-P_\infty}{\frac{1}{2}\rho.U_\infty^2} \quad (7)$$

In Eq. (7), Cp represents the pressure coefficient, P the pressure at the point, P_∞ the free-flow pressure, and ρ the specific mass of the fluid.

Equation (8) represents Reynolds number.

$$\mathrm{Re} = \frac{\rho.V.L}{\mu} \quad (8)$$

Strouhal Number (St) represents the dominant frequency of vortices and establishes a relationship between the frequency of detachment of a pair of vortices, the characteristic linear size and the velocity of the flow. It is an important parameter to determine the critical velocity for vortex detachment. St is calculated according to Eq. (9) or through Fig. 5, as quoted by Lienhard, 1966, and Achenback, 1981.

$$St = \frac{f.D}{U_\infty} \quad (9)$$

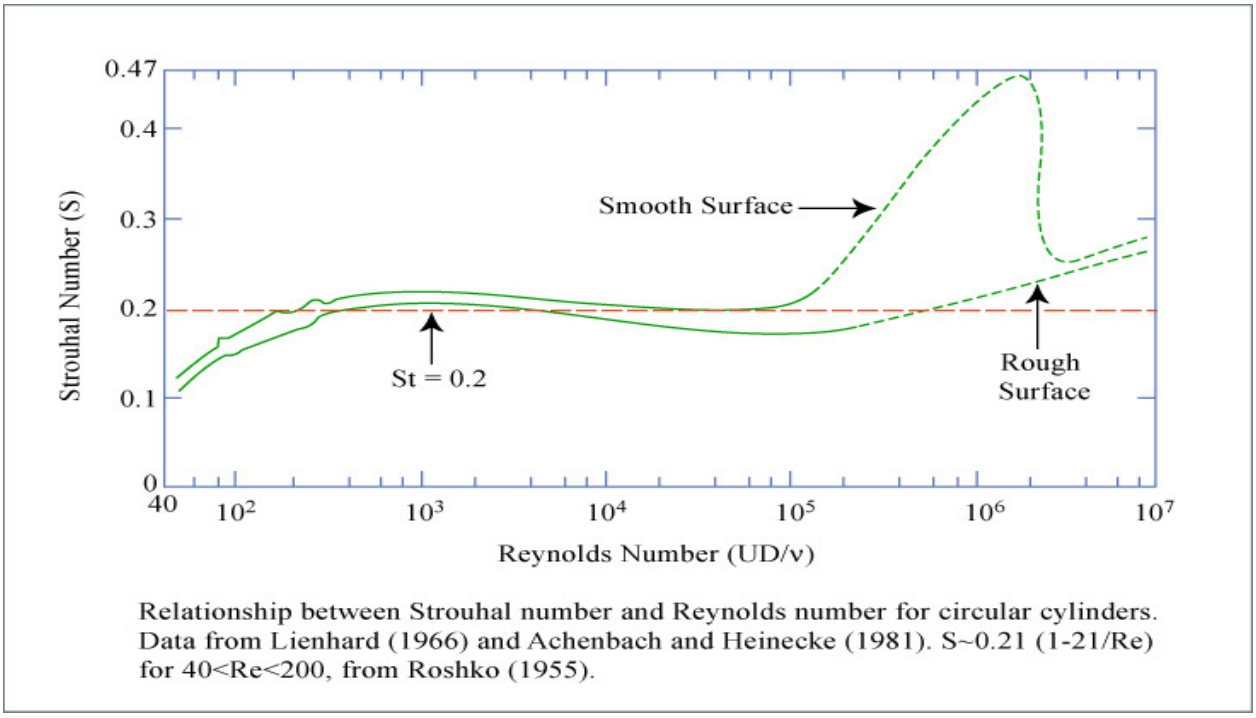

Figure 5. Strouhal number x Reynolds number for circular cylinders.
Adapted from Lienhard, 1966, and Achenback, 1981.

Klopfenstein (1998) developed Eq. (10), valid for ideal gas conditions, which aimed to convert the dynamic pressure into velocity.

$$V = 44{,}72136.\, k_{Pitot}.\, \Gamma_{Pitot} \sqrt{\frac{\Delta P.f}{\rho}} \tag{10}$$

3. RESULTS

The mesh was generated through the Ansys Meshing 18.2 software. The meshes generated contained prismatic elements in the wall, aiming a better calculation in the boundary layer regions, and tetrahedral elements in the free-flow region. According to Çengel and Cimbala (2007), meshing is one of the most important parameters in a CFD simulation.

The dimensionless wall distance parameter (Y Plus) was introducing by Von Kármán for his universal wall law for turbulent boundary layers. For the SST model, the ideal values of Y+ should be inferior than 1 (ANSYS, 2017).

A Re = 0.89274 10^5 was found, Eq. (8), and then, through Fig. (3), a value of St = 0.2. Then, this value of St was used to find the correct Timestep for the transient simulation, which is equal to 0.002 or less.

Residue and mesh tests were performed for a rotation of 2500 rpm. In steady state, four different meshes were evaluated, progressively increasing the number of nodes and elements. For each mesh, pressure and velocity values were compared at points 1 and 2, as indicated in Fig. 6.

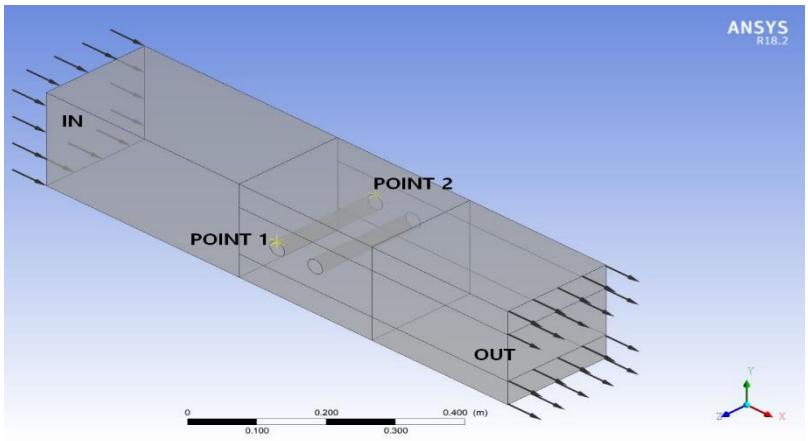

Figure 6. Solution convergence assessment points

When the values of velocity and pressure in the evaluated points did not change within a set limit, it was considering that the problem converged and this procedure was repeating for meshes that are more refined. When the converged results of a mesh no longer changed significantly when compared to the ones from a more refined mesh, it considered that the problem converged. (ANSYS, 2017). Tab. (1) presents the results of the residues and meshes tests.

Table 1. Convergence of meshes

Meshes and Y Plus	Convergence	Number of elements	Number of nodes	Velocity (m/s) Point 1	Pressure (Pa) Point 2
Mesh 1	10^{-4}	1053094	357016	0.7600	-21.51
	10^{-5}			0.7207	-23.84
0.978223	10^{-6}			0.7210	-23.79
Mesh 2	10^{-4}	4244447	1174811	0.4327	-25.95
	10^{-5}			0.4419	-26.21
0.605131	10^{-6}			0.4426	26.19
Mesh 3	10^{-4}	8160204	2038022	0.4082	-24.26
	10^{-5}			0.4137	-24.32
0.530053	10^{-6}			0.4136	-24.33
Mesh 4	10^{-4}	10778254	2783589	0.4184	-24.27
	10^{-5}			0.4186	-24.66
0.456965	10^{-6}			0.4193	-24.67

Figure 7 shows a detail of the mesh 4 in the region near the wall of the test section having a minimum element size of 0.0012 mm. The mesh was composed of tetrahedral and prismatic elements, in order to know the flow near the walls.

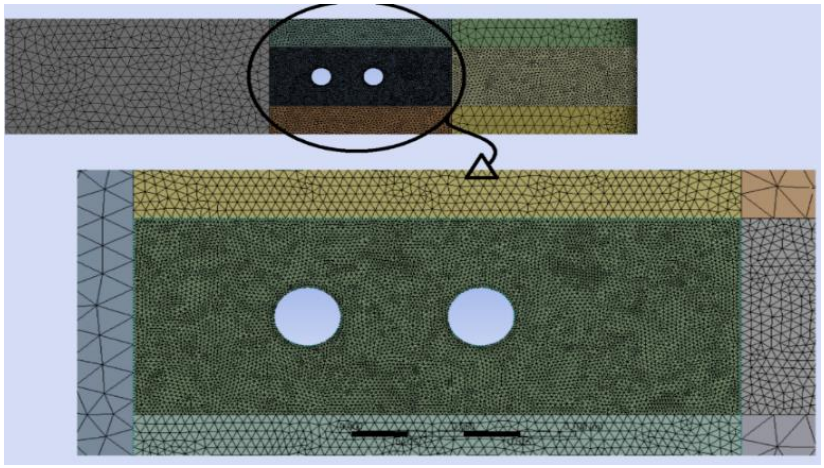

Figure 7. Mesh of cylinders used

Figure 8 shows the pressure plane along the test section. A favorable pressure gradient upstream of the cylinder and an adverse pressure gradient downstream thereof and around cylinder 2 are clearly apparent. This pressure differential causes the separation of the flow, as indicated by White (2011). The cylinder 1 has an upstream pressure gradient of 42.817 Pa and a downstream pressure of -88.219 Pa, a pressure differential of 131,036 Pa. On the other hand, cylinder 2, upstream pressure has a value of 7.125 Pa and downstream of -15.649, therefore, a pressure differential of 22.774 Pa.

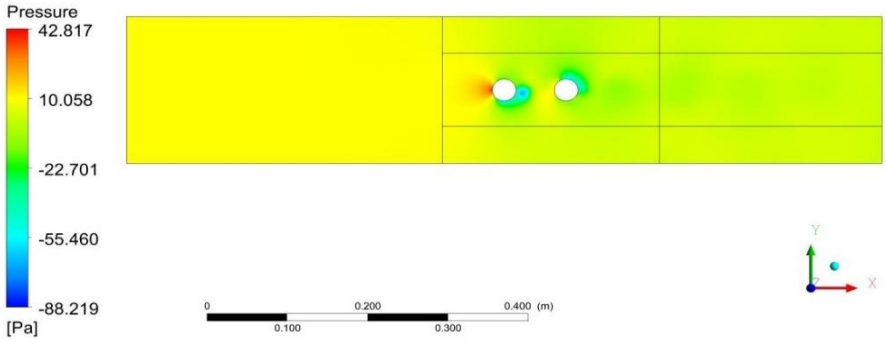

Figure 8. Pressure plane.

Figure 9 shows the Velocity plane along the test section. Note that after each of the two cylinders, vortices are forming due to the generation of wakes, as shown by Zdravkovich (1984 and 1988). There is an increase in velocity at the respective points of separation of each of the two cylinders, caused by the frictional force with the surface of the cylinder that has less influence on the flow. The minimum velocity is observed at the stagnation point , where the upstream flow of the first cylinder occurs, leading to a zero velocity. In turbulent regimes there are still oscillatory moments due to the release of the generated vortices, which explains the minimum velocity also found in other points of the wakes. According to Soares (2013), the flow profile in the test section is not completely developing, so the velocity at the center of the tunnel is approximately uniform. With the insertion of the two cylinders in the test section, an increase of the flow velocity occurs until reaching its registered maximum speed of 13.66 m/s.

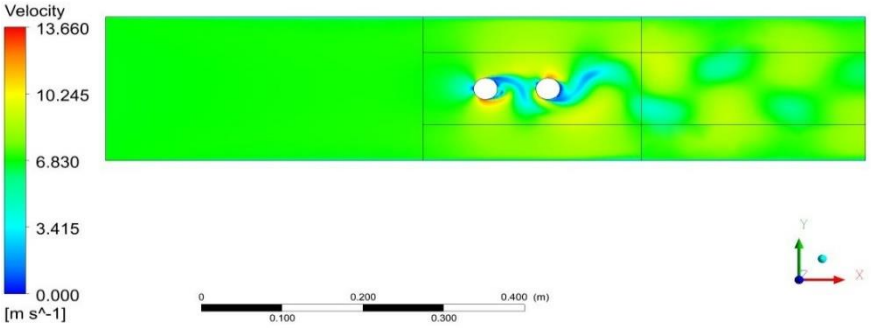

Figure 9. Velocity plane.

Figure 10 shows pressure coefficient versus angle of attack of cylinders 1 and 2. The behavior of the curve is in accordance with Incropera et al. (2017). For cylinder 1, the value of 1.2325 found as a pressure coefficient, with a boundary layer detachment in the cylinder by about 87°. For the cylinder 2, Cp = -0.7 was found, the separation having an angle of about 113°, corroborating with literature found in White (2011).

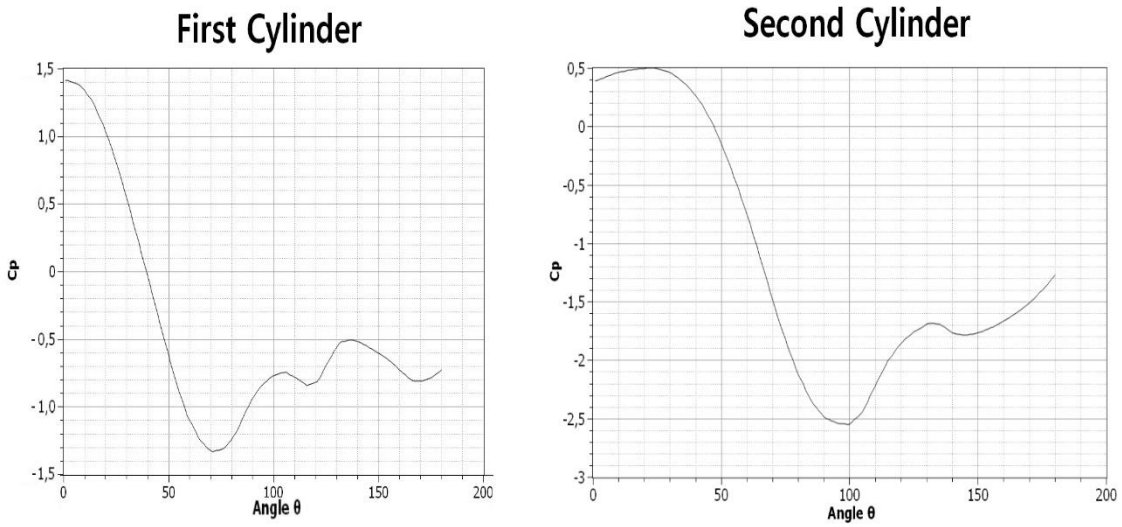

Figure 10. Coefficient of Pressure x Angle θ.

Figure 11 shows the Wall Shear x Angle θ curve for the cylinders 1 and 2. Noted that the detachment of the boundary layer for cylinder 1 is confirmed at 87° and for cylinder 2 at 113°

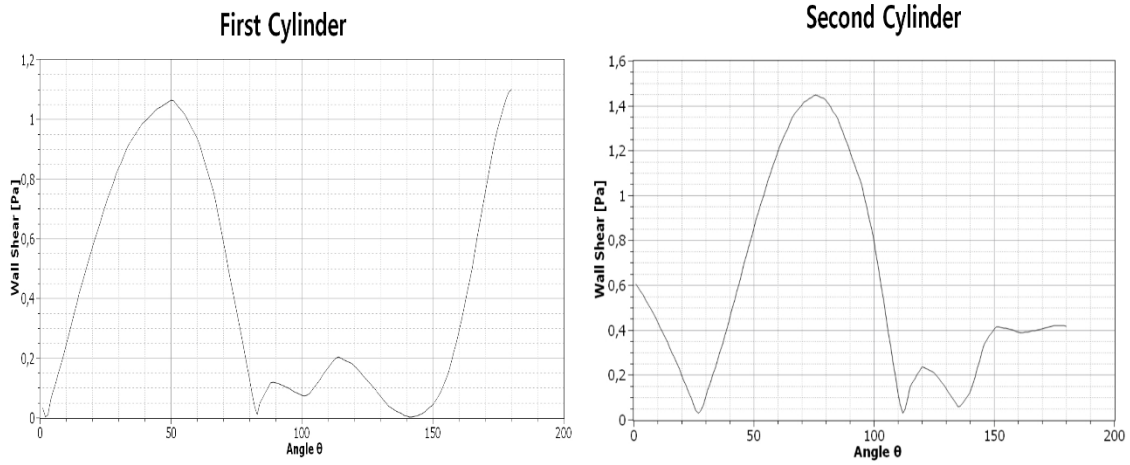

Figure 11. Wall Shear x Angle θ.

The drag force on the cylinder can be determined using Eq. (4). The existence of a trailing force can be perceive in the direction of flow by the pressure difference between the sides of the cylinder. Using the drag coefficient for the laminar flow around 1.2, Cengel and Cimbala (2015) cylinders, they obtained a value of 0.997 N for drag. For the solution of the problem's governing equations, the Reynolds number was used based on the hydraulic diameter of the test section (0.2 m of edges) and temperature of 20ºC for specific mass of the air (1.205 kg/m^3) and absolute viscosity (1.82 x 10^5 kg/s.m). Considering as turbulent the flow with Re greater than 4000. The value for the Re of 8.9274 x 10^4 found. However, to evaluate the flow around the cylinders, the Re used based on its diameters, with a found value of 1.3257 x 10^4. Thus, the flow was considered turbulent and the value calculated for drag was F_d= 0.196 N.

The validation of a numerical simulation and subsequent use of its results returned by the solver are only be done from comparisons with experimental results (OBERKAMPF; TRUCANO; HIRSCH, 2004). In this work, the verification performed from points mapped at the output of the section of tests and compared numerically and experimentally. Fig. 12 shows the velocity curves found experimentally and numerically.

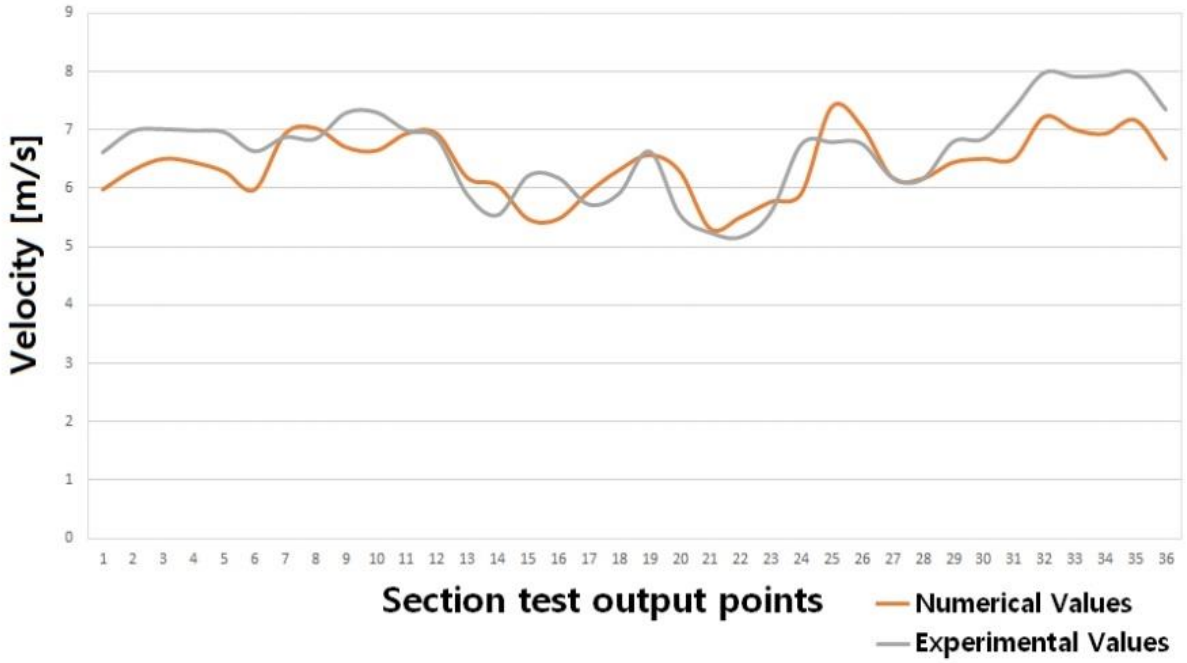

Figure 12. Velocity at the test section output with experimental and numerical values

The experimental uncertainty of the data is state to be the range in which the actual measurement value is find. This measure should contain 95% reliability. Considering this reliability value, any experimental analysis are basing on three aspects: accuracy, precision and significant numbers (WHITE, 2011).

The value of uncertainty found was ± 0.3 m/s. For the volumetric flow rate, uncertainty was approximately ± 0.002 m^3/s due to the velocities found in the test. Then flow rate calculated at the outputs of the test sections being 0.246 ± 0.002 m^3/s.

The calculations of the uncertainties of the results with the tube of Pitot followed recommendations of ISO 3966 (2013), where it is emphasized the importance of knowing the degree of uncertainty of the values of dynamic pressure measured with the tube of Pitot and other variables of influence in the measurement process (BRAZILIAN ASSOCIATION OF TECHNICAL STANDARDS, 2013). Small deviations are observe in the values find. For Piot tube tests, all sources of errors related to the results are in obtaining the differential pressure, due to fluctuations at low speeds, in the specific mass of the fluid; In calculating the compressibility factor of the fluid, in the Pitot tube calibration, due to turbulence, due to the transverse velocity gradient, due to the blockage of the conduit, due to the inclination of the Pitot tube in relation to the flow, due to the loss of load between total and static pressure take-off and due to test temperature.

4. CONCLUSION

In this work, numerical simulations of the flow inside a wind tunnel for low speeds realized, with the insertion of two circular cylinders. The main conclusions were that a favorable pressure gradient upstream of cylinder 1 and adverse pressure gradients downstream of the same cylinder and cylinder 2 observed, causing flow detachment and wake formation. The detachment point occurred at an angle of approximately 87° for the first cylinder and 120° for the second. When comparing the velocity fields for one and two cylinders inserted in the test section, it perceived that proximity and wake interference and reinsertion of the quasi-constant wake occur. The Prandtl-type Pitot tube collected the results for the wind tunnel, where the velocity data validated the numerical work.

5. ACKNOWLEDGEMENTS

This study was financed in part by the Coordenação de Aperfeiçoamento de Pessoal de Nível Superior - Brasil (CAPES).

The authors would also like to thank the Pontifícia Universidade Católica de Minas Gerais (PUC Minas), the Fundação de Amparo à Pesquisa do Estado de Minas Gerais (FAPEMIG), the Conselho Nacional de Desenvolvimento Científico e Tecnológico (CNPq).

6. REFERENCES

Achebach, E. and Heinecke, E, 1981."On Vortex Shedding from Smooth and Rough Cylinders in the Range of Reynolds Numbers 6x10^3 to 5x10^6"; *Journal of Fluid Mechanics*, Vol 109, PP.239-251.

Ansys, 2017. "CFX Solver Theory manual". Version 18.2.

Associação brasileira de normais técnicas, 2013. NBR ISO 3966: "Medição de vazão em condutos fechados — Método velocimétrico utilizando tubos de Pitot estático". Rio de Janeiro.

Çencel, Y.; Cimbala, J., 2015. "Mecânica dos Fluidos: Fundamentos e Aplicações". 3. ed. São Paulo: McGraw-Hill, 896 p..

Fox, R. W.; Pritchard, P. J.; Mcdonald, A.T., 2010. "Introdução à mecânica dos fluidos." 7. ed. Rio de Janeiro: LTC - Livros Técnicos e Científicos, 710p.

Gusberti, V.; Vielmo, H.; Severo, D., 2004. "Análise e Melhoramento de um Ventilador Axial Através de Simulação Numérica". *In: Congresso nacional de engenharia mecânica*, Belém-PA. Anais do CONEM. Rio de Janeiro: Associação Brasileira de Engenharia e Ciências Mecânicas.

Hill, R. R.; Ahner, D. L.; Dillard, D. A.; Montgomery, D. C., 2018. "Examining potential reductions in wind tunnel testing requirements". Volume 34, Issue7 *Special Issue: The ENBIS-17 Quality and Reliability Engineering International*. November 2018 Pages 1363-1373.

Incropera, F. P; Bergman, T. H.; Lavine, A. S.; Dewitt, D. P., 2017. "Fundamentos de transferência de calor e de massa". 7. ed. Rio de Janeiro: LTC, 2017. Rio de Janeiro: LTC.

Klopfenstein, R. Jr., 1998. "Air velocity and flow measurement using a pitot tube". ISA Transactions, V. 37, p. 257-263.

Lienhard, J. H., 1966. "Synopsis of lift, drag and vortex frequency data for rigid circular cylinders". Dept. of Mechanical Engineering. Technical Extension Service. Washington University, Pullman, Washington.

Menter, F. R., 1992. "Influence of freestream values on κ-ω turbulence model predictions". *American Institute of Aeronautics and Astronautics Journal*, v. 30, n. 6, pp. 1657-1659.

Oberkampf, W. L.; Trucano, T. G.; Hirsch, C., 2004. "Verification, validation, and prectivecabability in computational engineering and physics". *Applied Mechanics and Materials*, v. 57, n 5, pp. 345-384.

Soares, C. B., 2008. "Estudo experimental do comportamento fluidodinâmico na seção de testes de um túnel de vento para baixas velocidades". 138 f. Dissertação (Mestrado) – Pontifícia Universidade Católica de Minas Gerais, Programa de Pós-Graduação em Engenharia Mecânica, Belo Horizonte.

Teo, Z. W.; New, T. H.; Li, S.; Pfeiffer, T,; Nagel, B.; Gollnick, V., 2018. "Wind tunnel testing of additive manufactured aircraft components", Rapid Prototyping Journal, Vol. 24 Issue: 5, pp.886-893, https://doi.org/10.1108/RPJ-06-2016-0103. Jan. 2018.

Vasconcellos, G. L. F. de., 2015. "Estudo numérico e experimental do escoamento ao redor de um cilindro circular em um túnel de vento para baixas velocidades". 146 f. Dissertação (Mestrado) – Pontifícia Universidade Católica de Minas Gerais, Programa de Pós-Graduação em Engenharia Mecânica, Belo Horizonte, 2015.

Versteeg, H K.; Malalasekera, W., 2007. "An Introduction to Computacional Fluid Dynamics – The Finite Volume" Method. 2ª Ed. Inglaterra: Pearson Education Limited.

White, F. M., 2011. "Mecânica dos Fluidos". 6 ed. Rhode Island: McGraw.

Wilcox, D. C., 2000, "Turbulence Modeling for CFD", 2nd, DCW Industries, Inc. La Cañada, Califórnia, EUA.

Xiang, H.; Lia, Y.; Chenb, S.; Lia, C., 2017. "A wind tunnel test method on aerodynamic characteristics of moving vehicles under crosswinds". School of Civil Engineering, Southwest Jiaotong University, Chengdu, Sichuan 610031, China and Department of Civil and Environmental Engineering, Colorado State University, Fort Collins, CO 80523, USA, Jan. 2017.

Zdravkocich, M. M., 1984. "Classification of flow-induced oscillations of two parallel circular cylinders in various arrangements". *ASME Winter Annual Meeting, Sym- posium on Flow-Induced Vibrations* 2, 1–18.

Zdravkocich, M. M., 1988. "Review of interference-induced oscillations in flow past two parallel circular cylinder in various arrangements". J. Wind Eng. Ind. Aerodyn. 28, 183–200.

7. RESPONSIBILITY NOTICE

The authors are the only responsible for the printed material included in this paper.